Speed-up of Diffusive Shock Acceleration and its implications for AGN and gamma-bursts

A. Begley, A. Meli, and J. J. Quenby

Astrophysics Group, Imperial College, London, SW7 2BZ, UK

Abstract

The rate of diffusive shock acceleration is considerably enhanced relative to that given by non-relativistic theory when the upstream plasma flow has a Lorentz factor of ten or more. This fact yields a major modification to the particle production in central accretion shocks of AGN. We compute the expected neutrino, neutron and gamma-ray output from regions within 100 Schwarzschild radii of the black hole with interactions of proton with photons and protons and neutrons with matter (including synchrotron losses) and find that by taking into account lower energy processes modifications are made to previous conclusions. The ability to see variability from this central engine via gamma-ray observations is discussed. We compute by Monte-Carlo method, shock acceleration rates for large Lorentz factors relevant to the cosmic fire-balls thought to produce gamma-bursts.

1 Sporadic Shock Model:

While gamma-ray production in AGN is often ascribed to synchrotron self-Compton photons arising from electron acceleration in the relativistic jet, neutrinos, if emitted, are most likely to come from the interactions of protons, accelerated by the shocks which may develop in the relativistic accretion flow expected near the central black hole. It is this latter model we examine here for both particle and photon production, following the work of Battersby, Drolias and Quenby (1995). To know the position, velocity and inclination of the accretion shock, we note Molteni, Lanzafame and Chakrabarti (1994) show that there is a unique position for a stable, spherical shock which is very sensitive to the angular momentum and internal energy of the plasma. This implies that a small variation in these parameters will disrupt the shock. The region where it is assumed these shocks develop would undoubtedly be highly inhomogeneous. Sporadic shocks would form when regions of lower and higher angular momentum collide at a radius $R = xR_s$ where $R_s = 2GM/c^2$ is the Schwarzchild radius. At different radii they produce spectra of protons with different maximum energies and spectral indices. If the accreting specific mass flux is proportional to its specific angular momentum $\dot{m}(\mathcal{L}) \propto \mathcal{L}$, there is an equal amount of kinetic energy flux through shocks per logarithmic interval of x. The luminosity contributions will then be weighted according to $L(x) \propto 1/x$, if the efficiency is the same for all shocks. We expect quasi-perpendicular shocks as the frozen in magnetic field is drawn out in the direction of motion of the plasma and these shocks will have de Hoffmann-Teller frame velocities of $u_1 \geq 0.5$. According to Lieu et al. (1994), computational simulations demonstrate a speed up of the diffusive shock acceleration time constant over the conventional value given by $t_{acc} = [c/(u_1 - u_2)][\lambda_1/u_1 - \lambda_2/u_2]$ by a factor of s up to a value of 10, where $\lambda_{1,2}$ are upstream and downstream mean free paths and $u_{1,2}$ are the flow velocities in the de Hoffmann-Teller frame. In this quasi- perpendicular model we use $N(E) \propto E^{-\gamma}$ with $\gamma \simeq 1.8$, to account for the spectral hardening found computationally, and a de Hoffmann-Teller velocity of $0.7c$.

2 Acceleration and Cooling Times:

By equating the time scales for acceleration and cooling we estimate the maximum proton energy. We use the above expression for first order Fermi acceleration time, t_{acc} with $\lambda = fR_g = fE/eB$, where R_g is the proton gyroradius, E is its energy, B is the magnetic field and f is the factor by which λ is increased over the Bohm limit. Valdés-Galicia, Quenby and Moussas (1992) show in the solar wind case f is large and a value of 40 is taken here. Assuming a strong shock, the compression ratio will be 4, then $t_{acc} = 20c\lambda/3su_1^2 \approx 2.96 \times 10^{-2} E_9/(sB\beta_1^2)$ sec. Here $\beta_1 = u_1/c$ and E_9 is the proton energy in units of $10^9 GeV$. The decrease

in acceleration time is offset by including the diffusion factor increase. From Stecker and Salamon (1996), $L_{UV} = L_x = 0.05L_{Edd}$ for AGN of all types and luminosities, thus setting $R_s = 4.6 \times 10^{13}L_{45}$ cm. ($L_{45} = L_{UV}$ or L_X in units of $10^{45}\mathrm{ergs}^{-1}$).

To estimate the dependance of the field on the luminosity and radius, we assume equipartition with radiation and a field frozen into the plasma, so $B \propto 1/R$. If the AGN mechanism is similar over eight orders of magnitude in luminosity we require a scaling to achieve equipartition, $B \propto L^{-0.5}$. The magnetic field energy is normalised to the X-ray energy density at $x = 5$. $B^2/8\pi = L_x/400\pi R_s^2 c \times 5/x$, then $B = 2800L_{45}^{-0.5}x^{-1}$G. This means that $t_{acc} \approx 1.05 \times 10^{-5}s^{-1}\beta_1^{-2}xL_{45}^{0.5}E_9$ sec. In the case of the quasi-perpendicular shock we take $\beta_1 = 0.7c$, $s = 8$, $t_{acc} = 2.69 \times 10^{-6}xL_{45}^{0.5}E_9$ sec.

For pγ cooling, $t_{p\gamma}^{-1} \approx N_\gamma\sigma_{p\gamma}c\kappa$ where N_γ is the number density of the photons above the threshold, κ is the inelasticity and $\sigma_{p\gamma} \approx 5 \times 10^{-28}$ cm^2 is the cross section at resonance, just above threshold, where all the interactions take place. Taking the UV and the X-ray photon density spectrum used by Stecker and Salamon (1996), (valid up to $x = 10$ and beyond this the spectrum decays as $1/R^2$).
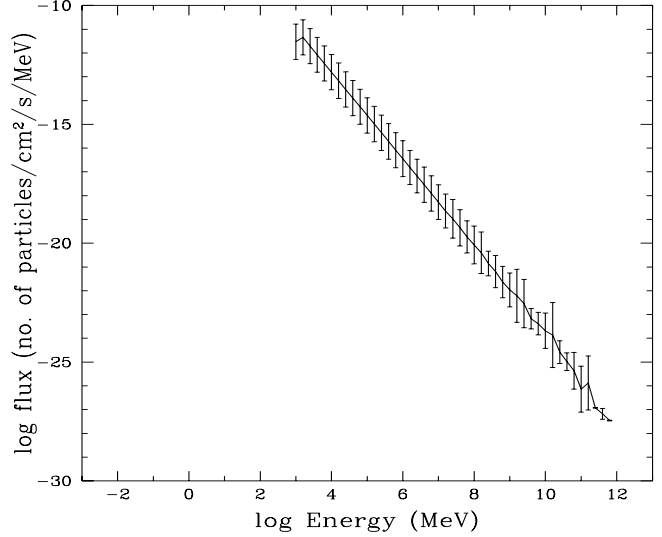

Figure 1: Shock accelerated proton spectrum, averaged over all shock radii.

$$n(\epsilon) \approx \frac{5 \times 10^{14}}{L_{45}}cm^{-3}eV^{-1} \times \begin{cases} 0.165\epsilon, & \epsilon < 1eV, \\ 0.165\epsilon^{-0.9}, & 1eV < \epsilon < 40eV, \\ 5.35 \times 10^{-5}\epsilon^2 e^{-\epsilon/15}, & 40eV < \epsilon < 192eV, \\ 4.15 \times 10^{-2}\epsilon^{-1.7}, & 192eV < \epsilon < 10^6 eV, \end{cases}$$

We include pp cooling, important at lower proton energies.

3   Photo-pion Production:

The protons react by $p + \gamma \to \Delta^+ \to p + \pi^0$ or $n + \pi^+$ and the neutrons by $n + \gamma \to \Delta^0 \to p + \pi^-$ or $n + \pi^0$. The pions then decay spontaneously $\pi^0 \to 2\gamma$, $\pi^+ \to \mu^+ + \nu_\mu$ with $\mu^+ \to e^+ + \nu_e + \overline{\nu}_\mu$ and $\pi^- \to \mu^- + \overline{\nu}_\mu$ with $\mu^- \to e^- + \overline{\nu}_e + \nu_\mu$. The energy is divided amongst the decay products so that energy in $\nu_\mu + \overline{\nu}_\mu$ and $\nu_e + \overline{\nu}_e$ is 0.4 and 0.2 times the energy in the electrons and the gamma-rays, respectively, when all the secondary protons and neutrons and reprocessed. If $\kappa_\pi^- \approx 0.2$ then the first generation of neutrinos have $E_\nu \approx E_p/20$ and each succeeding generation has 0.8 times the energy of the last. For $\gamma < 2$ most of the energy in the neutrinos is near $E_{\nu(max)}$.

4   The Secondary Fluxes:

The total secondary particle and photon flux for an AGN from the central engine model is calculated from the contribution from all radii.

The resulting spectrum is normalised to the X-ray emission, taking the non thermal X-ray fraction as 20%, consistent with some soft gamma-ray observations (Zdziarski, 1994). We essentially assume spherically symmetric production. The initial proton spectrum (figure 1, normalised as are all subsequent figures for 3C273 to fluxes which would notionally reach the Earth) is followed on an individual particle basis, relativistically, putting in isotropic magnetic scattering. Secondary pion production in the photon field is followed into γ, ν and $e^{\pm}$ and the subsequent cascade γ and synchrotron photons computed, allowing especially for $\gamma\gamma$ interactions. The secondary neutron flux and significant consequent cascade is also followed. Addition of pp scattering and the convection of lower energy primary protons into the black hole are important effects. Much of the secondary output is due to shocks close to $100R_s$.
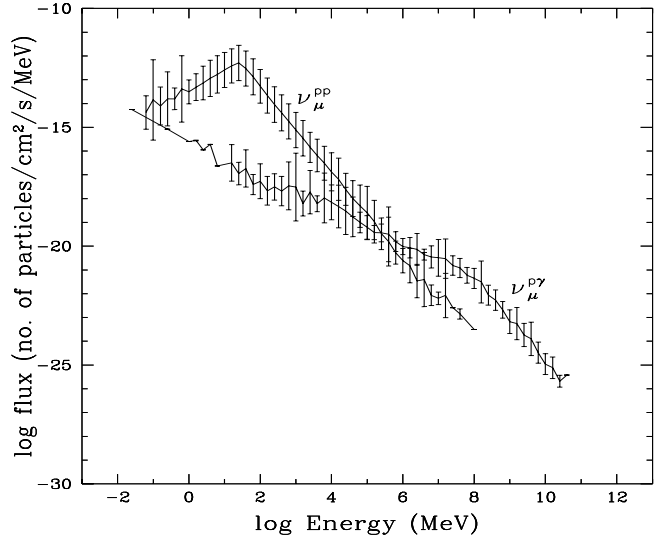

Figure 2: Neutrino spectrum, flux at Earth from 3C273. Production by pp and $p\gamma$ are shown with the total energy in ν_{μ}^{pp} being one tenth the energy in $\nu_{\mu}^{p\gamma}$

5   Resulting Neutrino, Neutron and Photon Output:

In figure 2 we show the predicted neutrino flux at Earth from the $p\gamma$ and pp chains and note the dominance of pp collisions below 10GeV not seen in our previous approximation (Battersby, Drolias and Quenby, 1995).

Figure 3 shows the pion and synchrotron contributions to the gamma flux, illustrating the dominance of synchrotron emission at all but the highest energies. Both in the GeV and TeV range, the predictions still fall short of typical AGN observations by ~ 100. Figure 4 shows the neutron flux before decay, the absolute numbers still do not seem sufficient to boost the gamma flux after decay to match observation without invoking some beaming mechanism involving 'catching' charged particles in the relativistic jets. It is necessary to see significant gamma output directly from sub $100R_s$ regions if the observed time variations in BL Lac AGN emission is to tell us about black hole physics rather than jet structure.
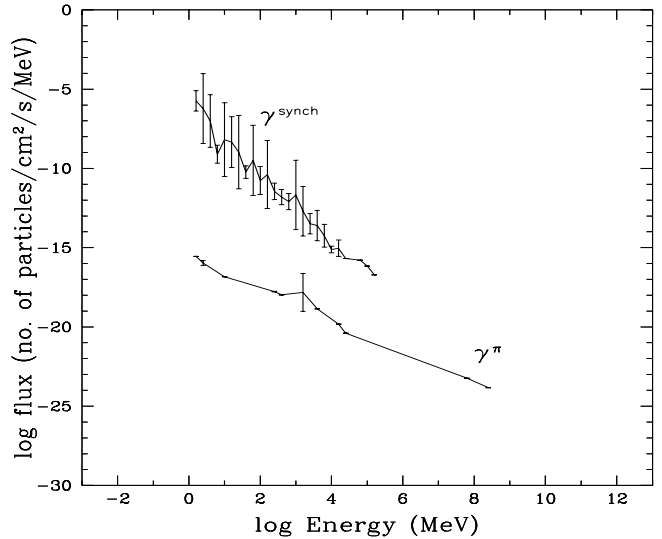

Figure 3: Gamma-ray spectrum from region $100R_s$ from central black hole. Contribution from synchrotron and π^0 decay are marked

6   Diffusive Shock Speed-up Simulations:

Vietri (1997), models gamma-bursts under the relativistic fire-ball model, where the relativistic shock has a Lorentz gamma factor ~ 1000, taking into account the relativistic speed-up (Quenby and Lieu, 1989) of diffusive shock acceleration. Just a few shock crossings produce ultra- relativistic protons whose synchrotron radiation should produce measurable γ fluxes up to 300 GeV. Here we consider the computations of Quenby
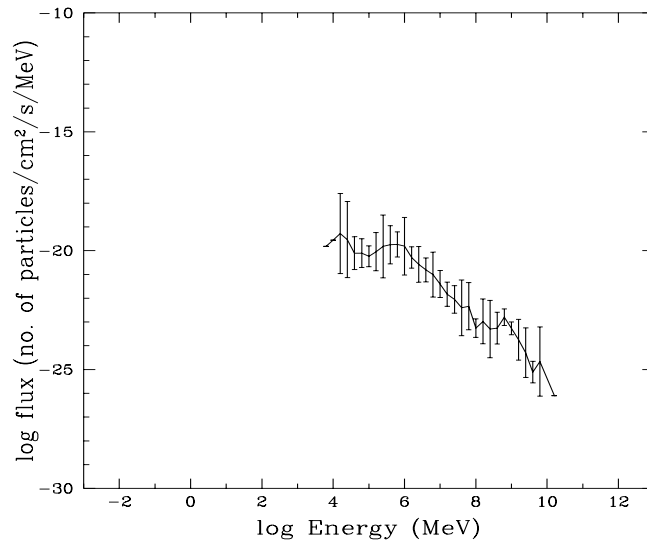
Figure 4: Escaping neutron spectrum, at $100R_s$ - flux normalized to flux at Earth.

and Lieu (1989) for parallel shocks, with isotropic scattering in the fluid frames, the most favourable case for allowing repeated transmission across the shock surface, to investigate the applicability of the speed-up to higher Lorentz factors. The guiding centre approximation is assumed with conservation of the first adiabatic invariant at the shock, compression ratio 4 and a rigidity dependent mean free path as in the previous work. An isotropic particle distribution is injected upstream and particles are removed far downstream. Scattering is according to $Pr(z) \sim \exp(-z/\lambda|\cos\theta|)$ for pitch angle θ.

Preliminary results for the upstream Lorentz factor in the range 10-35, yield differential spectral slopes close to 1. If we define 'speed-up' as the ratio of the measured time constant for particle acceleration at Lorentz factors close to the plasma speed based on Monte-Carlo simulation to that predicted by the non-relativistic flow expression mentioned in section 2, preliminary results find the ratio ~ 0.1 to 0.3 in the above γ range, thus supporting the importance of this effect in supplying the highest energy accelerated particles in AGN and gamma-burst scenarios.

References

Battersby, S.J.R., Drolias, B. and Quenby, J.J. 1995, Astrop. Phys. 4, 151

Lieu, R., Quenby, J.J., Drolias, B. and Naidu, K. 1994, ApJ 421, 211

Molteni, D., Lanzafame, G. and Chakrabarti, S.K. 1994, ApJ 425, 161

Quenby, J.J. and Lieu, R. 1989, Nature 342, 654

Stecker, F.W. and Salamon, M.H. 1996, Space Science Rev. 75, 341

Valdés-Galicia, J.F., Quenby, J.J., Moussas, X. 1992, Solar Phys 139, 189

Vietri, M. 1997, Phys. Rev. Lett. 78, 4328

Zdziarski, A.A. 1994, The Second Compton Symposium, eds. Fichtel, C.E. et al. 525